

www.acsnano.org

# New Growth Frontier: Superclean Graphene

Jincan Zhang, Luzhao Sun, Kaicheng Jia, Xiaoting Liu, Ting Cheng, Hailin Peng,\* Li Lin,\* and Zhongfan Liu\*



Downloaded via SOOCHOW UNIV on November 16, 2024 at 03:52:51 (UTC). See https://pubs.acs.org/sharingguidelines for options on how to legitimately share published articles

Cite This: ACS Nano 2020, 14, 10796-10803

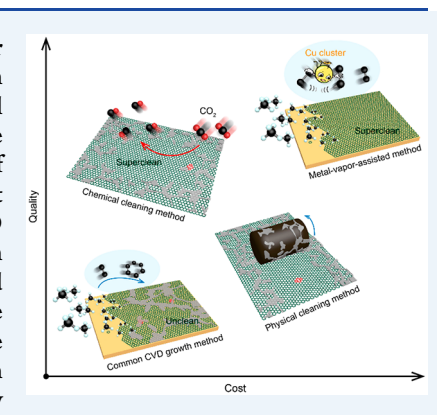


**ACCESS** I

Metrics & More

Article Recommendations

ABSTRACT: The last 10 years have witnessed significant progress in chemical vapor deposition (CVD) growth of graphene films. However, major hurdles remain in achieving the excellent quality and scalability of CVD graphene needed for industrial production and applications. Early efforts were mainly focused on increasing the single-crystalline domain size, large-area uniformity, growth rate, and controllability of layer thickness and on decreasing the defect concentrations. An important recent advance was the discovery of the inevitable contamination phenomenon of CVD graphene film during high-temperature growth processes and the superclean growth technique, which is closely related to the surface defects and to the peeling-off and transfer quality. Superclean graphene represents a new frontier in CVD graphene research. In this Perspective, we aim to provide comprehensive understanding of the intrinsic growth contamination and the experimental solution of making superclean graphene and to provide an outlook for future commercial production of high-quality CVD graphene films.



raphene has emerged as one of most promising materials due to its fascinating and extraordinary properties.<sup>1,2</sup> Since it was first isolated, significant developments in graphene synthesis methodologies have progressed,3 among which chemical vapor deposition (CVD) holds appealing potential for graphene mass production with outstanding quality, controllability, and scalability. Efforts to increase the domain size, uniformity, and growth rate continue; however, a gap remains between the outstanding properties of mechanically exfoliated graphene and those of CVD graphene. In this regard, as unveiled in recent research, the surface contamination that is inevitably introduced during CVD growth might be the Achilles' heel of CVD graphene; such contamination is closely related to lattice defects and has detrimental effects on the intrinsic properties and performance of graphene products. Going beyond efforts to remove airborne contamination and transfer-related impurities, 7,8 an ideal solution would be rooted in the removal of contamination formed in the CVD process, which would ensure a clean graphene surface after the transfer and exposure to the air. Understanding contamination phenomena and developing strategies for growing superclean graphene represent a new frontier of CVD graphene research. The formation mechanism of surface contamination needs to be elucidated to develop superclean growth techniques. In this Perspective, we first focus on contamination formation mechanisms in CVD and highlight the importance of synthesizing superclean graphene. After reviewing the state-of-the-art superclean growth strategies, we outline the future directions and opportunities

concerning the industrial production of high-quality superclean graphene films.

# INEVITABLE CONTAMINATION FORMED DURING HIGH-TEMPERATURE GROWTH

Contamination on graphene surfaces can be categorized as (1) amorphous carbon, containing a large number of distorted hexagon, pentagon, and heptagon rings of carbon atoms, formed during high-temperature growth; (2) transfer-related polymer residues, which are left on the graphene surface after the transfer due to the difficulty in removing macromolecular polymers; (3) airborne contamination, such as hydrocarbons from the ambient air, which can significantly alter the wettability of graphene.<sup>7</sup> Contamination can occur during the growth, transfer, and storing processes. However, suppressing the formation of amorphous carbon during CVD growth to grow clean graphene then reduces transfer-related and airborne contamination afterward, highlighting the key importance of removing amorphous carbon to prepare superclean graphene surfaces. In the following sections, we

Published: August 25, 2020





discuss the formation mechanism of amorphous carbon and related superclean growth strategies.

Understanding contamination phenomena and developing strategies for growing superclean graphene represent a new frontier in chemical vapor deposition graphene research.

The synthesis of target materials coincides with the formation of byproducts with lower crystalline quality or even amorphous structures. Such side reactions are influenced by the synthesis parameters, such as catalyst, temperature, and reactant concentration. As discussed in the preparation of synthetic graphite, carbon nanotubes (CNTs), and diamond, the generation of amorphous carbon can occur on the surface of target carbon materials or in the gas phase. <sup>10,11</sup> For instance, the formation of amorphous carbon was widely observed on the surfaces of CNTs, which is fueled by produced carbon species in the gas phase. <sup>12</sup>

During CVD growth of graphene on Cu, the formation of amorphous carbon with two-dimensional (2D) structures is also observable on the graphene surface. Both surface reactions and gas-phase reactions occur during high-temperature CVD growth and are responsible for the formation of amorphous carbon. In detail, the introduction of carbon precursors into the high-temperature chamber initiates the decomposition of carbon feedstock on catalytic metal substrates to produce active carbon species (e.g., CH<sub>3</sub>, CH<sub>2</sub>, and CH on Cu surfaces). Subsequently, these carbon species may be consumed by the nucleation or growth of graphene through on-surface diffusion and attachment (Figure 1a). However, carbon species can also desorb into the gas phase and alter the gas-phase reactions. Such carbon species would further evolve into larger carbon clusters, such as C<sub>4</sub>H<sub>2</sub>, C<sub>4</sub>H<sub>4</sub>,  $C_4H_6$ ,  $C_5H_5$ ,  $C_6H_6$ ,  $C_7H_8$ ,  $C_8H_5$ ,  $C_8H_6$ ,  $C_8H_8$ , and  $C_{10}H_8$ , through radical reactions in the gas phase. <sup>14,15</sup> Consequently, accumulation of carbon species (from C1 species to larger carbon clusters) in the gas phase persists during CVD growth (Figure 1a). 15,10

In turn, the adsorption of the active carbon species and carbon clusters existing in the gas phase occurs onto either the metal surfaces or as-formed graphene. Carbon species that are adsorbed on uncovered metal foil decompose into basic carbon species, catalyzed by Cu.<sup>5</sup> In contrast, such decomposition becomes difficult on the graphene surface because the coverage of graphene suppresses the catalytic ability of Cu. With a higher diffusion barrier, the direct deposition of larger carbon clusters on a graphene surface directly results in the nucleation of amorphous carbon (Figure 1b).<sup>17</sup> Similar to the nucleation of graphene on Cu, such clusters should contain sufficient carbon atoms to stabilize and immobilize themselves on graphene surface.<sup>5</sup> In the case of smaller carbon species, however, these small species move on the surface of graphene and collisions between them initiate the nucleation of amorphous carbon. Specifically, lattice defects in graphene may function as active sites for nucleation because such defects have stronger interactions with the active carbon species and carbon clusters. After nucleation, amorphous carbon captures the moving carbon species on graphene and the carbon species from the gas phase to fuel its lateral growth (Figure 1c). Finally, the full coverage of graphene significantly suppresses the catalytic ability of Cu, and almost no carbon species are produced; therefore, the growth of amorphous carbon almost ends completely after the full coverage of graphene. Overall, a reasonable growth process of amorphous carbon on the graphene surface includes three steps: (I) accumulation of active carbon species and carbon clusters in the gas phase, (II) nucleation of amorphous carbon on the surface of graphene, and (III) lateral growth of amorphous carbon (Figure 1).

The suppressed catalytic ability of Cu is responsible for the formation of amorphous carbon on the graphene surface. The evaporation of Cu also leads to the presence of Cu catalysts in the gas phase, especially in low-pressure CVD, because the temperature for growing graphene is near the melting point of Cu. In general, the decomposition barriers of carbon species either in the gas phase or on the graphene surface are highly reduced with the assistance of Cu vapor. The Cu-vapor-assisted decomposition of carbon species and as-formed amorphous carbon inhibits the formation of amorphous carbon on graphene. In addition, the Cu vapor facilitates the healing of the graphene lattice and therefore reduces the number of active defective sites that may serve as nucleation sites of amorphous carbon. However, the Cu vapor is usually insufficient, even in low-pressure growth, due to its low-

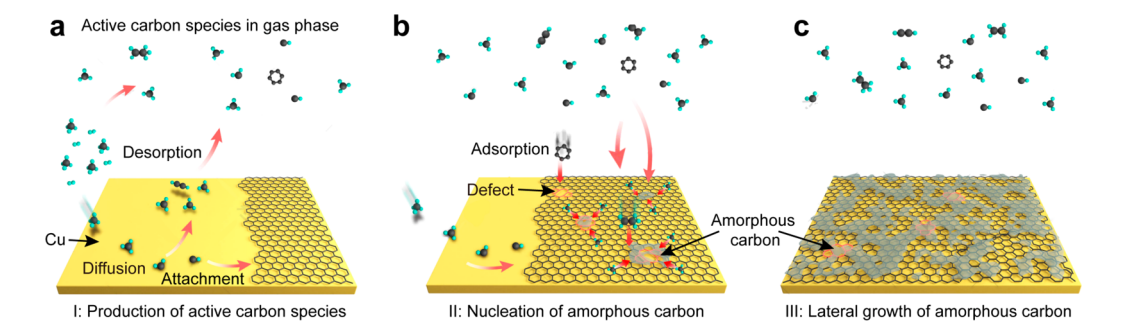


Figure 1. Schematics of the formation mechanism of amorphous carbon on the graphene surface during high-temperature growth. (a) Production of active carbon species. The decomposition of carbon precursors on Cu leads to the production of active carbon species; some of the produced carbon species may be consumed by the growth of graphene through on-surface diffusion and attachment, whereas others may desorb into the gas phase, resulting in the presence of plenty of carbon species in the gas phase (step I). (b) Nucleation of amorphous carbon. The adsorption of active carbon species on the graphene surface initiates the nucleation of amorphous carbon. Nucleation occurs primarily at the defective sites of graphene (step II). (c) Lateral growth of amorphous carbon. The moving carbon species on the graphene surface and carbon species from the gas phase fuel the lateral growth of amorphous carbon (step III).

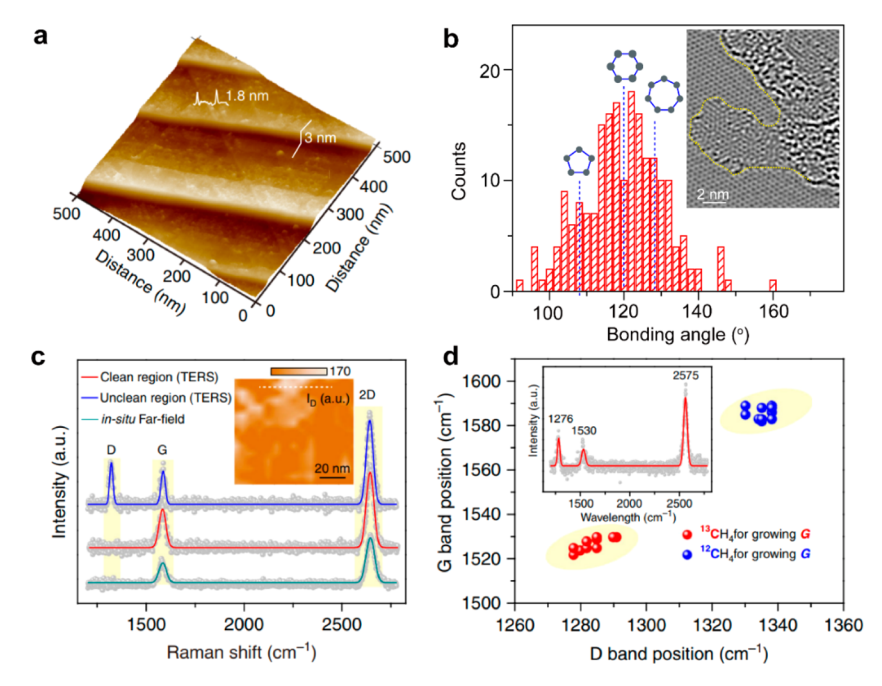


Figure 2. Inevitable contamination on the surface of chemical vapor deposition (CVD)-derived graphene films. (a) Atomic force microscopy image of graphene on Cu foil directly after growth. (a) Reproduced with permission from ref 9. Copyright 2019 Springer Nature. (b) Statistics of C–C bond angles in amorphous carbon obtained from corresponding high-resolution transmission electron microscopy (HRTEM) image. Inset: HRTEM image of unclean graphene. (b) Reproduced with permission from ref 18. Copyright 2019 Wiley-VCH. (c) Tip-enhanced Raman spectra (TERS) of the unclean (blue line) and clean (red line) regions in unclean graphene sample and *in situ* far-field Raman spectrum of graphene (dark cyan line). Inset: TERS mapping of the D band intensity. (d) Statistics of the D and G band positions from the contaminated regions of graphene grown by <sup>12</sup>CH<sub>4</sub> (blue) and <sup>13</sup>CH<sub>4</sub> (red). Inset: Representative TERS spectra of isotopically labeled graphene. (c,d) Reproduced with permission from ref 9. Copyright 2019 Springer Nature.

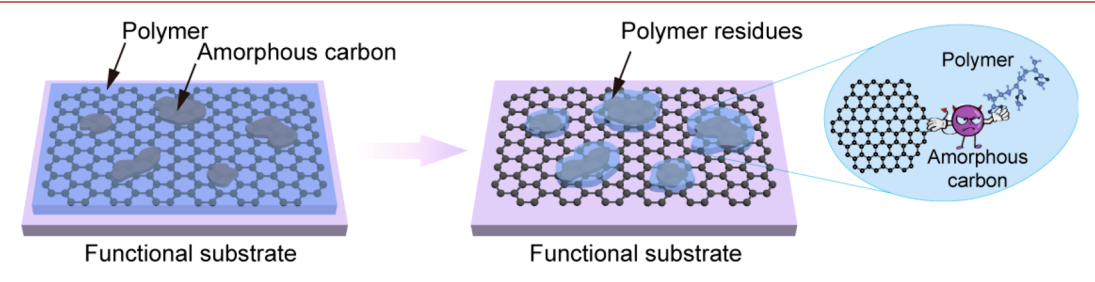


Figure 3. Schematic illustration of contamination in the transfer of graphene onto functional substrates. After polymer removal, polymer residues are left on the graphene regions that are covered by amorphous carbon because of the strong interaction between amorphous carbon and polymer.

saturation vapor pressure ( $<3 \times 10^{-7}$  bar at  $\sim 1000$  °C). Furthermore, Cu evaporation is gradually suppressed with the increasing coverage of graphene, escalating the insufficiency of the Cu catalyst in the gas phase.

Our group recently showed that contamination on the graphene surface originates in high-temperature growth. In atomic force microscopy (AFM) images of graphene on the Cu surface after growth, surface contamination is observed, occupying over 50% area of the entire region with thicknesses ranging from 0.3 to 3.2 nm (Figure 2a). The universal distribution of contamination on the graphene surface is also confirmed by high-resolution transmission electron microscopy (HRTEM) images, where the sizes of continuous clean regions are smaller than 100 nm. Notably, the contamination is composed of a large number of distorted hexagons, pentagons, and heptagons and exhibits a nearly 2D nature (Figure 2b). A conjunction of the tip-enhanced Raman spectrum (TERS) with isotope labeling techniques also indicates that the surface

contamination is mainly amorphous carbon with a strong D band (Figure 2c,d).

After growth, the graphene needs to be transferred from metal substrates to functional substrates for further device fabrication and applications. Polymers, such as poly(methyl methacrylate) (PMMA), are usually used as the transfer medium to protect the graphene from breakage. However, the strong interactions between polymers and amorphous carbon through dangling bonds cause polymer residues to be left on the graphene surface after transfer (Figure 3). In other words, unclean graphene covered by an abundance of amorphous carbon is likely to become even more dirty after transfer. Ph. 18,21,22 In contrast, nearly no contamination is observed on the surface of CVD-grown superclean graphene films after transfer, confirming the importance of growing superclean graphene.

Table 1. Properties of Superclean Graphene and Graphene Grown by Common Methods<sup>9</sup>

		superclean graphene	graphene grown by common methods
electrical properties	carrier mobility	17,000 cm <sup>2</sup> ·V <sup>-1</sup> ·s <sup>-1</sup> (room temperature) 31,000 cm <sup>2</sup> ·V <sup>-1</sup> ·s <sup>-1</sup> (1.9 K)	11,000 cm <sup>2</sup> ·V <sup>-1</sup> ·s <sup>-1</sup> (room temperature) 17,800 cm <sup>2</sup> ·V <sup>-1</sup> ·s <sup>-1</sup> (1.9 K)
	contact resistance	115 Ω·μm	351 Ω·μm
	sheet resistance	$272 \Omega \cdot \text{sq}^{-1}$	410 $\Omega \cdot \text{sq}^{-1}$
optical property	optical transmittance	97.6% at 550 nm	97.0% at 550 nm
thermal property	thermal conductivity	3230 $\text{W} \cdot \text{m}^{-1} \cdot \text{K}^{-1}$ 2420 $\text{W} \cdot \text{m}^{-1} \cdot \text{K}^{-1}$	
wettability water contact angle		40°	65°

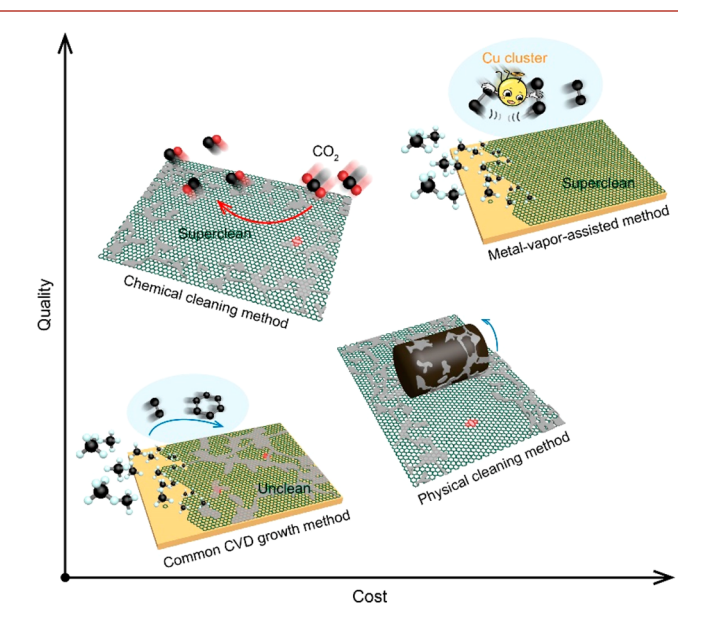
# TOWARD CHEMICAL VAPOR DEPOSITION GROWTH OF HIGH-OUALITY GRAPHENE FILMS

Only graphene with compelling structural features will enable us to realize truly competitive applications of graphene. Thus, the commercial applications of CVD graphene should stand on the basis of growth of high-quality graphene. Unrelenting efforts have been devoted to achieving fine control over the domain size, layer number, doping configuration, and flatness of CVD graphene in recent years: the domain size of graphene has increased from micrometer-size scales to meter sizes in the past 10 years;<sup>23</sup> monolayer graphene, AB-stacking bilayer, and ABA-stacking trilayer graphene were recently synthesized in controllable manners; 24,25 ultraflat single-crystal graphene wafers with wrinkle-free surfaces (Ra < 0.5 nm) were also successfully grown on both Cu and CuNi single-crystal and record-breaking graphene conductivity has been achieved in millimeter-size nitrogen-cluster-doped graphene single crystals.<sup>28</sup> Nevertheless, the properties of CVD-grown graphene are still not comparable to those of mechanically exfoliated graphene.<sup>5</sup> One key reason lies in the inevitable surface contamination on the surface of CVD-grown graphene film, which will strongly influence its optical, thermal, mechanical, and electrical properties.<sup>2</sup>

Little attention has been paid to the impact of growthrelated contamination on the performance of graphene, although there is broad consensus that polymer residues would strongly degrade the properties of graphene films.8, Relying on the availability of superclean graphene films free of amorphous carbon, Liu's group systematically compared the properties of graphene grown by common methods and superclean graphene. Superclean graphene exhibits outstanding electrical, optical, and thermal properties after the removal of amorphous carbon and polymer residues (Table 1). For example, the contact resistance of superclean graphene is comparable to the values of mechanically exfoliated graphene samples, due to the strengthened coupling between the contact metal and graphene. Superclean graphene encapsulated by hexagonal boron nitride exhibits ultrahigh carrier mobilities  $(1,083,000 \text{ cm}^2 \cdot \text{V}^{-1} \cdot \text{s}^{-1} \text{ for electrons and } 625,000 \text{ cm}^2 \cdot \text{V}^{-1} \cdot \text{s}^{-1}$ for holes, at 1.9 K), higher than previously reported values of CVD-grown graphene films, highlighting the importance of superclean graphene growth.

# STRATEGIES FOR MAKING SUPERCLEAN GRAPHENE

Based on the above discussion, the accumulation of active carbon species and carbon clusters in the gas phase is mainly responsible for the formation of amorphous carbon. The metal catalysts in the gas phase can promote the decomposition of large carbon species and clusters into small carbon species, suppressing the nucleation of amorphous carbon and facilitating the healing of graphene defects (Figure 4). Cu foam, with its porous structure and high specific surface area,



Methods	Cleanness	Defects	Scalability	Cost
Common CVD growth method	***	***	****	****
Chemical cleaning method	****	****	****	****
Physical cleaning method	****	<b>**</b> *	****	****
Metal-vapor-assisted method	****	****	****	****

Figure 4. Comparison of the current experimental methods for preparing superclean graphene in terms of quality, cost, cleanness, defect density, and scalability.

would supply more Cu catalysts to suppress the formation of amorphous carbon during high-temperature growth. The large-scale growth of superclean graphene film was successfully realized using alternating Cu foil and Cu foam stacks. Similarly, using metal-containing carbon feedstock is another strategy to introduce additional Cu catalysts in the gas phase to promote the decomposition of large carbon clusters and, therefore, to suppress the formation of amorphous carbon. For example, the growth of superclean graphene film was achieved using copper(II) acetate, Cu(OAc)<sub>2</sub>, as the carbon source. <sup>21</sup>

In addition to modification of the gas-phase reactions during the high-temperature process, the preparation of superclean graphene can be achieved through chemical reactions with the as-formed amorphous carbon on the graphene surface, such as selective etching. Appropriate etchant and reaction parameters are required to achieve selective etching without producing damage to the graphene lattice. Fortunately, CO<sub>2</sub>, as a moderate oxidizer, was reported to be capable of reacting

with amorphous carbon at  $\sim$ 500 °C without generating new defects. <sup>18</sup>

Superclean graphene exhibits outstanding electrical, optical, and thermal properties after the removal of amorphous carbon and polymer residues.

Inspired by household lint rollers and brooms, physical removal of surface contaminants is also feasible because interactions between the amorphous carbon and the underlying graphene are in the form of weak van der Waals forces. With a porous structure and rich functional groups, activated carbon was shown to be efficient in removing surface contamination through its strong interactions with amorphous carbon.<sup>21</sup> The control of interfacial force is essential in this method.

Superclean graphene films produced from the above methods exhibit differences in quality, cost, and scalability. Graphene synthesized by the metal-vapor-assisted CVD method exhibits the highest quality because catalysts in the gas phase contribute to the healing of metastable defects during the growth. However, the production capacity of graphene films using this method is limited. Specifically, the

inevitable fusion that occurs between the Cu foam and Cu foil at high temperatures should be resolved for further mass production. As a solid carbon source, the quantity of Cu(OAc)<sub>2</sub> used for growing graphene needs to be carefully controlled to achieve uniformity, especially in a large-scale CVD system. In contrast, postgrowth treatments, including CO<sub>2</sub> selective etching and the activated-carbon-coated lint roller, are compatible with many current growth techniques and can easily be scaled up for mass production in a costefficient manner. However, some issues remain to be resolved before mass production can begin. For example, the removal of amorphous carbon is spatially inhomogeneous, especially when cleaning graphene on hard or rough substrates, due to poor contact. Furthermore, because postgrowth methods cannot heal the intrinsic defects produced during the CVD growth process, the quality of the as-obtained graphene still must be improved (Figure 4).

#### CONCLUSION AND PROSPECTS

Surface contamination is a major hurdle to probing the intrinsic properties of CVD graphene and to realizing its mass production with compelling quality. We predict that superclean graphene will represent a new frontier of graphene research in the near future.

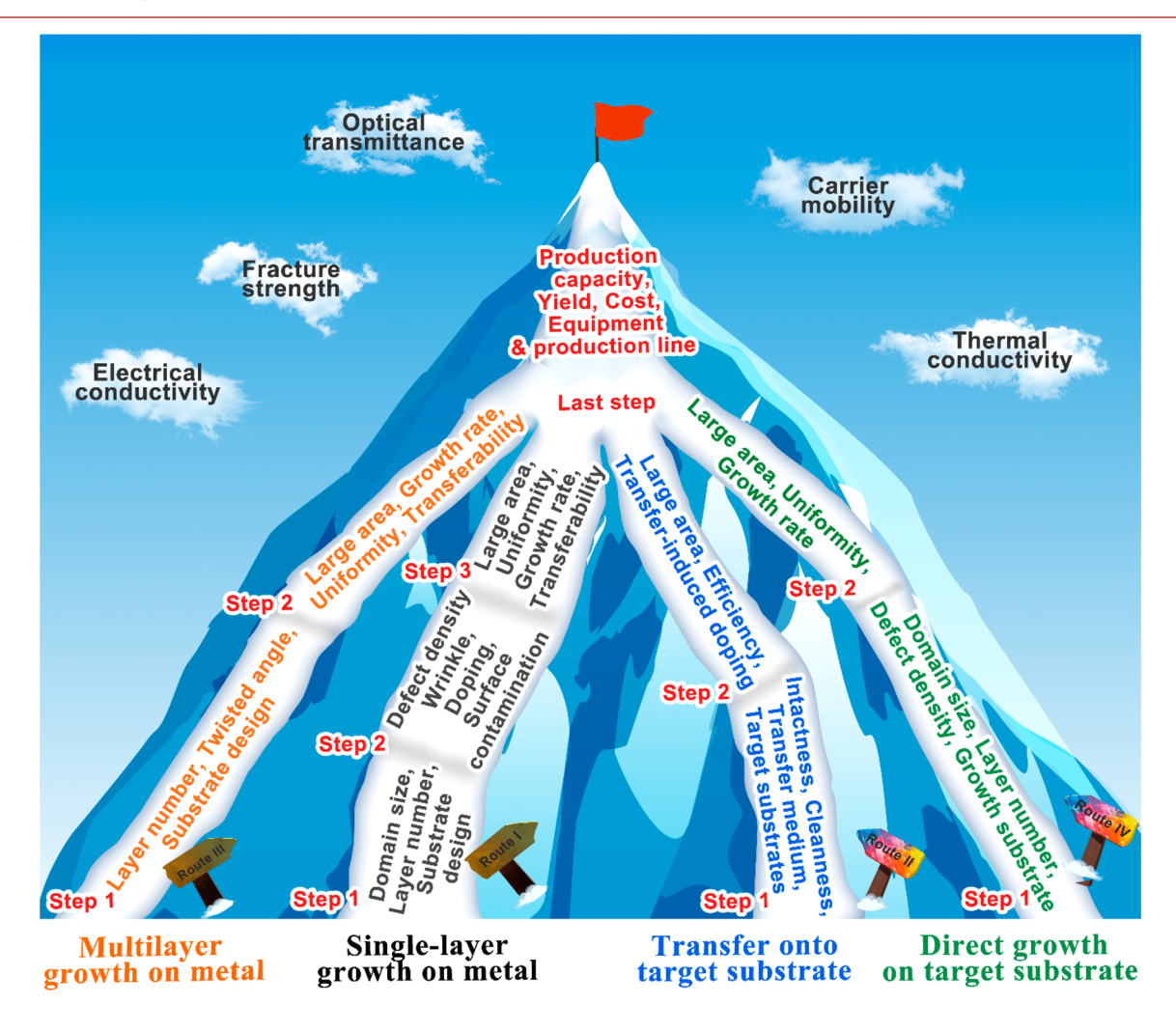


Figure 5. Challenges for mass production of chemical vapor deposition graphene.

Low-cost, large-area production of superclean, defect-free graphene with good uniformity is essential for industrial applications but remains challenging. Based on the formation mechanisms of the amorphous carbon, three aspects should be considered when developing new strategies for making superclean graphene: (1) suppressing the formation of large carbon clusters in the boundary layer, possibly by tuning the thickness and content of the boundary layer; (2) healing defects, which would reduce the number of the nucleation sites of amorphous carbon on the graphene surface; (3) suppressing the lateral growth of amorphous carbon on the graphene surface. Furthermore, theoretical calculations with deeper insights into the formation mechanism of amorphous carbon and techniques for visualizing the defects and amorphous carbon are also urgently needed.

As new approaches are developed, their compatibility with current techniques should also be taken into consideration. 5,23 For instance, graphene single-crystal wafers (GSCWs) are currently considered to be one of the important commercial categories of graphene products for electronics-grade applications, due to its appealing quality and flatness. The growth of GSCWs on thin Cu(111) films is usually conducted in an atmospheric pressure CVD system to prevent the evaporative loss of Cu. However, the increased pressure and reduced Cu vapor in the boundary layer significantly alters the gas-phase reactions and affects the cleanness of the as-grown graphene. Therefore, in this case, a trade-off between cleanness and flatness should be made.

The industrial production of graphene relies on advances in both production facilities and quality improvements because production needs to change dramatically from the laboratory to the industrial scale. In particular, because the formation of amorphous carbon is sensitive to the amount of catalyst and carbon species in the gas phase, the spatial distributions of gas and temperature are critical for the growth of superclean graphene. Therefore, both the mass and heat transfer will influence the quality and uniformity of as-produced graphene films and deserve more attention in mass production.<sup>3</sup> Furthermore, finite-element simulations should be conducted when designing the key components of high-end industrial CVD systems. In addition, a cold-wall CVD system might be a promising alternative due to its mass and heat transfer and the fact that, in this system, the sample size would not be limited by the diameter of the quartz tube.

A summary roadmap of CVD graphene with a view toward the mass production of high-quality graphene films is presented in Figure 5, where four routes represent the mainstream of current graphene research: the CVD growth of monolayer graphene on metal substrates (route 1), the transfer of graphene onto functional substrates (route 2), direct CVD growth of graphene on functional substrates (route 3), and CVD growth of multilayer graphene on metal substrates (route 4). In all of the routes, three or four steps are required to go from basic laboratory-scale fundamental research to industry-scale production of graphene. For example, in the first stage of route 1, main concerns for the graphene community are control over the structural features of CVD graphene, including domain size and layer number. In the meantime, the design of suitable substrates for controllable, cost-efficient mass production has also ignited intense research activity. In the subsequent stage, the main efforts of graphene researchers and the industrial community are currently devoted to issues of surface contamination, including defects, wrinkles,

and doping. Afterward, in the third stage, industrially feasible production strategies will be widely discussed with special emphasis on uniformity, size, growth rate, and transferability of graphene films. At the last stage, challenges for mass production and commercialization remain to be tackled, covering the production capacity, yield, cost, equipment, and production line at the industrial scale.

The growth of superclean graphene will attract great attention in the near future because the availability of a clean surface would offer enhanced properties and performance of CVD graphene and facilitate the discovery of new applications. We believe that superclean graphene will bring us more exciting findings in fundamental research and promote the progress of the entire graphene industry.

# **AUTHOR INFORMATION**

#### **Corresponding Authors**

Zhongfan Liu — Center for Nanochemistry, Beijing Science and Engineering Center for Nanocarbons, Beijing National Laboratory for Molecular Sciences, College of Chemistry and Molecular Engineering, Peking University, Beijing 100871, People's Republic of China; Beijing Graphene Institute (BGI), Beijing 100095, People's Republic of China; orcid.org/0000-0003-0065-7988; Email: zfliu@pku.edu.cn

Li Lin — School of Physics and Astronomy, University of Manchester, Manchester M13 9PL, United Kingdom; Email: linli-cnc@pku.edu.cn

Hailin Peng — Center for Nanochemistry, Beijing Science and Engineering Center for Nanocarbons, Beijing National Laboratory for Molecular Sciences, College of Chemistry and Molecular Engineering, Peking University, Beijing 100871, People's Republic of China; Beijing Graphene Institute (BGI), Beijing 100095, People's Republic of China; orcid.org/0000-0003-1569-0238; Email: hlpeng-cnc@pku.edu.cn

# Authors

Jincan Zhang — Center for Nanochemistry, Beijing Science and Engineering Center for Nanocarbons, Beijing National Laboratory for Molecular Sciences, College of Chemistry and Molecular Engineering, Peking University, Beijing 100871, People's Republic of China; Beijing Graphene Institute (BGI), Beijing 100095, People's Republic of China

Luzhao Sun — Center for Nanochemistry, Beijing Science and Engineering Center for Nanocarbons, Beijing National Laboratory for Molecular Sciences, College of Chemistry and Molecular Engineering, Peking University, Beijing 100871, People's Republic of China; Beijing Graphene Institute (BGI), Beijing 100095, People's Republic of China

Kaicheng Jia — Center for Nanochemistry, Beijing Science and Engineering Center for Nanocarbons, Beijing National Laboratory for Molecular Sciences, College of Chemistry and Molecular Engineering, Peking University, Beijing 100871, People's Republic of China; Beijing Graphene Institute (BGI), Beijing 100095, People's Republic of China

Xiaoting Liu — Center for Nanochemistry, Beijing Science and Engineering Center for Nanocarbons, Beijing National Laboratory for Molecular Sciences, College of Chemistry and Molecular Engineering and Academy for Advanced Interdisciplinary Studies, Peking University, Beijing 100871, People's Republic of China; Beijing Graphene Institute (BGI), Beijing 100095, People's Republic of China

Ting Cheng – Center for Nanochemistry, Beijing Science and Engineering Center for Nanocarbons, Beijing National

Laboratory for Molecular Sciences, College of Chemistry and Molecular Engineering and Academy for Advanced Interdisciplinary Studies, Peking University, Beijing 100871, People's Republic of China; Beijing Graphene Institute (BGI), Beijing 100095, People's Republic of China

Complete contact information is available at: https://pubs.acs.org/10.1021/acsnano.0c06141

#### **Author Contributions**

<sup>¶</sup>J.Z., L.S., and K.J. contributed equally.

#### Notes

The authors declare no competing financial interest.

# **ACKNOWLEDGMENTS**

This work was supported by Beijing National Laboratory for Molecular Sciences (BNLMS-CXTD-202001). This work was financially supported by the Beijing Municipal Science & Technology Commission (Nos. Z181100004818001 and Z191100000819005), the National Basic Research Program of China (No. 2016YFA0200101), and the National Natural Science Foundation of China (Nos. 51520105003 and 21525310).

#### **REFERENCES**

- (1) Reiss, T.; Hjelt, K.; Ferrari, A. C. Graphene Is On Track To Deliver On its Promises. *Nat. Nanotechnol.* **2019**, *14*, 907–910.
- (2) Lin, L.; Peng, H.; Liu, Z. Synthesis Challenges for Graphene Industry. *Nat. Mater.* **2019**, *18*, 520–524.
- (3) Novoselov, K. S.; Fal'ko, V. I.; Colombo, L.; Gellert, P. R.; Schwab, M. G.; Kim, K. A Roadmap for Graphene. *Nature* **2012**, *490*, 102, 200
- (4) Li, X. S.; Cai, W. W.; An, J. H.; Kim, S.; Nah, J.; Yang, D. X.; Piner, R.; Velamakanni, A.; Jung, I.; Tutuc, E.; Banerjee, S. K.; Colombo, L.; Ruoff, R. S. Large-Area Synthesis of High-Quality and Uniform Graphene Films on Copper Foils. *Science* **2009**, 324, 1312—1314.
- (5) Lin, L.; Deng, B.; Sun, J.; Peng, H.; Liu, Z. Bridging the Gap Between Reality and Ideal in Chemical Vapor Deposition Growth of Graphene. *Chem. Rev.* **2018**, *118*, 9281–9343.
- (6) Cheng, H. Superclean Graphene Films. Wuli Huaxue Xuebao 2020, 36, 1909042-0.
- (7) Li, Z. T.; Wang, Y. J.; Kozbial, A.; Shenoy, G.; Zhou, F.; McGinley, R.; Ireland, P.; Morganstein, B.; Kunkel, A.; Surwade, S. P.; Li, L.; Liu, H. T. Effect of Airborne Contaminants on the Wettability of Supported Graphene and Graphite. *Nat. Mater.* **2013**, *12*, 925–931.
- (8) Zhang, Z. K.; Du, J. H.; Zhang, D. D.; Sun, H. D.; Yin, L. C.; Ma, L. P.; Chen, J. S.; Ma, D. G.; Cheng, H. M.; Ren, W. C. Rosin-Enabled Ultraclean and Damage-Free Transfer of Graphene for Large-Area Flexible Organic Light-Emitting Diodes. *Nat. Commun.* **2017**, 8, 14560.
- (9) Lin, L.; Zhang, J. C.; Su, H. S.; Li, J. Y.; Sun, L. Z.; Wang, Z. H.; Xu, F.; Liu, C.; Lopatin, S.; Zhu, Y. H.; Jia, K. C.; Chen, S. L.; Rui, D. R.; Sun, J. Y.; Xue, R. W.; Gao, P.; Kang, N.; Han, Y.; Xu, H. Q.; Cao, Y.; et al. Towards Super-Clean Graphene. *Nat. Commun.* **2019**, *10*, 1912.
- (10) Hata, K.; Futaba, D. N.; Mizuno, K.; Namai, T.; Yumura, M.; Iijima, S. Water-Assisted Highly Efficient Synthesis of Impurity-Free Single-Walled Carbon Nanotubes. *Science* **2004**, *306*, 1362–1364.
- (11) Krasnikov, D. V.; Kuznetsov, V. L.; Romanenko, A. I.; Shmakov, A. N. Side Reaction in Catalytic CVD Growth of Carbon Nanotubes: Surface Pyrolysis of a Hydrocarbon Precursor with the Formation of Lateral Carbon Deposits. *Carbon* **2018**, *139*, 105–117.
- (12) Schunemann, C.; Schaffel, F.; Bachmatiuk, A.; Queitsch, U.; Sparing, M.; Rellinghaus, B.; Lafdi, K.; Schultz, L.; Buchner, B.; Rummeli, M. H. Catalyst Poisoning by Amorphous Carbon during

- Carbon Nanotube Growth: Fact or Fiction? ACS Nano 2011, 5, 8928-8934.
- (13) Chen, X. D.; Chen, Z. L.; Sun, J. Y.; Zhang, Y. F.; Liu, Z. F. Graphene Glass: Direct Growth of Graphene on Traditional Glasses. *Wuli Huaxue Xuebao* **2016**, 32, 14–27.
- (14) Wu, P.; Zhang, W.; Li, Z.; Yang, J. Mechanisms of Graphene Growth on Metal Surfaces: Theoretical Perspectives. *Small* **2014**, *10*, 2136–2150.
- (15) Lewis, A. M.; Derby, B.; Kinloch, I. A. Influence of Gas Phase Equilibria on the Chemical Vapor Deposition of Graphene. *ACS Nano* **2013**, *7*, 3104–3117.
- (16) Trinsoutrot, P.; Rabot, C.; Vergnes, H.; Delamoreanu, A.; Zenasni, A.; Caussat, B. The Role of the Gas Phase in Graphene Formation by CVD on Copper. *Chem. Vap. Deposition* **2014**, *20*, 51–58.
- (17) Jia, K. C.; Ci, H. N.; Zhang, J. C.; Sun, Z. T.; Ma, Z. T.; Zhu, Y. S.; Liu, S. N.; Liu, J. L.; Sun, L. Z.; Liu, X. T.; Sun, J. Y.; Yin, W. J.; Peng, H. L.; Lin, L.; Liu, Z. F. Superclean Growth of Graphene Using Cold-Wall Chemical Vapor Deposition Approach. *Angew. Chem., Int. Ed.* 2020, DOI: 10.1002/anie.202005406.
- (18) Zhang, J. C.; Jia, K. C.; Lin, L.; Zhao, W.; Huy, T. Q. A.; Sun, L. Z.; Li, T. R.; Li, Z. Z.; Liu, X. T.; Zheng, L. M.; Xue, R. W.; Gao, J.; Luo, Z. T.; Rummeli, M. H.; Yuan, Q. H.; Peng, H. L.; Liu, Z. F. Large-Area Synthesis of Superclean Graphene *via* Selective Etching of Amorphous Carbon with Carbon Dioxide. *Angew. Chem., Int. Ed.* **2019**, *58*, 14446–14451.
- (19) Chen, M.; Haddon, R. C.; Yan, R.; Bekyarova, E. Advances in Transferring Chemical Vapour Deposition Graphene: A Review. *Mater. Horiz.* **2017**, *4*, 1054–1063.
- (20) Chen, Y.; Gong, X. L.; Gai, J. G. Progress and Challenges in Transfer of Large-Area Graphene Films. Adv. Sci. 2016, 3, 1500343.
- (21) Jia, K. C.; Zhang, J. C.; Lin, L.; Li, Z. Z.; Gao, J.; Sun, L. Z.; Xue, R. W.; Li, J. Y.; Kang, N.; Luo, Z. T.; Rummeli, M. H.; Peng, H. L.; Liu, Z. F. Copper-Containing Carbon Feedstock for Growing Superclean Graphene. *J. Am. Chem. Soc.* **2019**, *141*, 7670–7674.
- (22) Sun, L. Z.; Lin, L.; Wang, Z. H.; Rui, D. R.; Yu, Z. W.; Zhang, J. C.; Li, Y. L. Z.; Liu, X. T.; Jia, K. C.; Wang, K. X.; Zheng, L. M.; Deng, B.; Ma, T. B.; Kang, N.; Xu, H. Q.; Novoselov, K. S.; Peng, H. L.; Liu, Z. F. A Force-Engineered Lint Roller for Superclean Graphene. *Adv. Mater.* 2019, 31, 1902978.
- (23) Zhang, J.; Lin, L.; Jia, K.; Sun, L.; Peng, H.; Liu, Z. Controlled Growth of Single-Crystal Graphene Films. *Adv. Mater.* **2020**, 32, No. 1903266.
- (24) Huang, M.; Bakharev, P. V.; Wang, Z. J.; Biswal, M.; Yang, Z.; Jin, S.; Wang, B.; Park, H. J.; Li, Y. Q.; Qu, D. S.; Kwon, Y.; Chen, X. J.; Lee, S. H.; Willinger, M. G.; Yoo, W. J.; Lee, Z.; Ruoff, R. S. Large-Area Single-Crystal AB-Bilayer and ABA-Trilayer Graphene Grown on a Cu/Ni(111) Foil. *Nat. Nanotechnol.* **2020**, *15*, 289–295.
- (25) Luo, D.; Wang, M. H.; Li, Y. Q.; Kim, C.; Yu, K. M.; Kim, Y. H.; Han, H. J.; Biswal, M.; Huang, M.; Kwon, Y.; Goo, M.; Camacho-Mojica, D. C.; Shi, H. F.; Yoo, W. J.; Altman, M. S.; Shin, H. J.; Ruoff, R. S. Adlayer-Free Large-Area Single Crystal Graphene Grown on a Cu(111) Foil. *Adv. Mater.* **2019**, *31*, No. 1903615.
- (26) Deng, B.; Pang, Z.; Chen, S.; Li, X.; Meng, C.; Li, J.; Liu, M.; Wu, J.; Qi, Y.; Dang, W.; Yang, H.; Zhang, Y.; Zhang, J.; Kang, N.; Xu, H.; Fu, Q.; Qiu, X.; Gao, P.; Wei, Y.; Liu, Z.; Peng, H. Wrinkle-Free Single-Crystal Graphene Wafer Grown on Strain-Engineered Substrates. ACS Nano 2017, 11, 12337–12345.
- (27) Zhang, X.; Wu, T.; Jiang, Q.; Wang, H.; Zhu, H.; Chen, Z.; Jiang, R.; Niu, T.; Li, Z.; Zhang, Y.; Qiu, Z.; Yu, G.; Li, A.; Qiao, S.; Wang, H.; Yu, Q.; Xie, X. Epitaxial Growth of 6 in. Single-Crystalline Graphene on a Cu/Ni (111) Film at 750 °C via Chemical Vapor Deposition. Small 2019, 15, No. 1805395.
- (28) Lin, L.; Li, J. Y.; Yuan, Q. H.; Li, Q. C.; Zhang, J. C.; Sun, L. Z.; Rui, D. R.; Chen, Z. L.; Jia, K. C.; Wang, M. Z.; Zhang, Y. F.; Rummeli, M. H.; Kang, N.; Xu, H. Q.; Ding, F.; Peng, H. L.; Liu, Z. F. Nitrogen Cluster Doping for High-Mobility/Conductivity Graphene Films with Millimeter-Sized Domains. *Sci. Adv.* **2019**, *5*, No. eaaw8337.

- (29) Chen, J. H.; Jang, C.; Xiao, S. D.; Ishigami, M.; Fuhrer, M. S. Intrinsic and Extrinsic Performance Limits of Graphene Devices on SiO<sub>2</sub>. *Nat. Nanotechnol.* **2008**, *3*, 206–209.
- (30) Pettes, M. T.; Jo, I. S.; Yao, Z.; Shi, L. Influence of Polymeric Residue on the Thermal Conductivity of Suspended Bilayer Graphene. *Nano Lett.* **2011**, *11*, 1195–1200.
- (31) Deng, B.; Liu, Z. F.; Peng, H. L. Toward Mass Production of CVD Graphene Films. *Adv. Mater.* **2019**, *31*, No. 1800996.